

Effect of Carbon Porosity on the Electrochemical Properties of Carbon/Polyaniline Supercapacitor Electrodes

M.A. Torre, C. del Río and E. Morales*

Instituto Ciencia y Tecnología de Polímeros (C.S.I.C.), c/ Juan de la Cierva 3, 28006 Madrid, Spain

Received: November 05, 2012, Accepted: December 13, 2012, Available online: July 04, 2013

Abstract: Supercapacitors have attracted great attention in power source applications, due to their high power density, elevated charge/discharge rate, good reversibility and long life. Activated carbons are the most frequently used electrode material, due to their high accessibility, non-toxicity, high chemical stability, good electrical conductivity, high surface area and low cost, but in practice the capacitance values are limited by the material microstructure. In this work we report on the synthesis and electrochemical characterization of carbon/polyaniline composites, synthesized by in-situ polymerization in acid media of aniline monomer on the surface of two activated carbons having different textural properties, and on the effect of the carbon porosity on the electrochemical properties of the electrodes. Results obtained indicate that the BET specific surface of the composites decreases sharply due to the collapse of the porous structure (mainly the micropores) of the carbon by the polyaniline chains. Regarding capacitance values, C_{sp} increases on increasing polyaniline loading in the composite, however high polymer concentration lead to a decrease on capacitance when high current were applied, probably due to diffusion restrictions of the electrolyte anions and cations to the carbon surface.

Keywords: Activated carbon, Polyaniline, Composite, Supercapacitor, Porosity, Specific capacitance

1. INTRODUCTION

Electrochemical capacitor devices, often called supercapacitors or ultracapacitors, have received significant attention in recent times due to their wide range of potential applications in hybrid electric vehicles, fuel cells, cellular phones, PDAs, etc [1-4]. Two types of mechanisms are associated with energy storage in a this kind of devices: one is the electric double-layer capacitor (EDLC), in which stored energy is accumulated by the separation of electronic and ionic charges at the interface between a high surface area electrode and an electrolyte solution; the other is the pseudocapacitor, in which the active species can be fast and reversibly oxidized and reduced at characteristic potentials. Carbon materials such as activated carbon fibers and powders, carbon aerogels, nanotubes [5-8]etc, are commonly used as electrode materials for EDLC, displaying good stability, but the capacitance values are limited by the slow ion transportation in the small micropores. Conducting polymers such as polyanilines (PANI's), polypyrroles (PPY's), polythiophenes (PT's), etc [9-11] and transition metal

oxides such as RuO₂, NiO, MnO₂, etc [12-14], have been used for redox capacitors. These devices generally display high capacitance, however conducting polymer based devices usually exhibit low stability during the charge/discharge process, while the high price of metal oxide restricts their commercial use.

Composites of carbons having different morphologies with conducting polymers or metal oxides can fully combine advantages of double-layer capacitance of the carbon with the pseudocapacitance of the redox material, providing electrodes with high specific capacitance and working voltage, but also excellent cycling stability [15-19]. Among conducting polymers, polyaniline (PANI) has been considered as one of the most promising candidate to be used, due to its high conductivity, ease of preparation, and good environmental stability [20-22]. In this work we report on the synthesis and electrochemical characterization of carbon/polyaniline composites, synthesized by in-situ chemical oxidative polymerization in acid media of aniline monomer on the surface of two commercial activated carbons having different textural properties, and on the effect of the carbon porosity on the electrochemical properties of the electrodes.

*To whom correspondence should be addressed: Email: emorales@ictp.csic.es
Phone: +34 915622900; Fax: +34 915644853

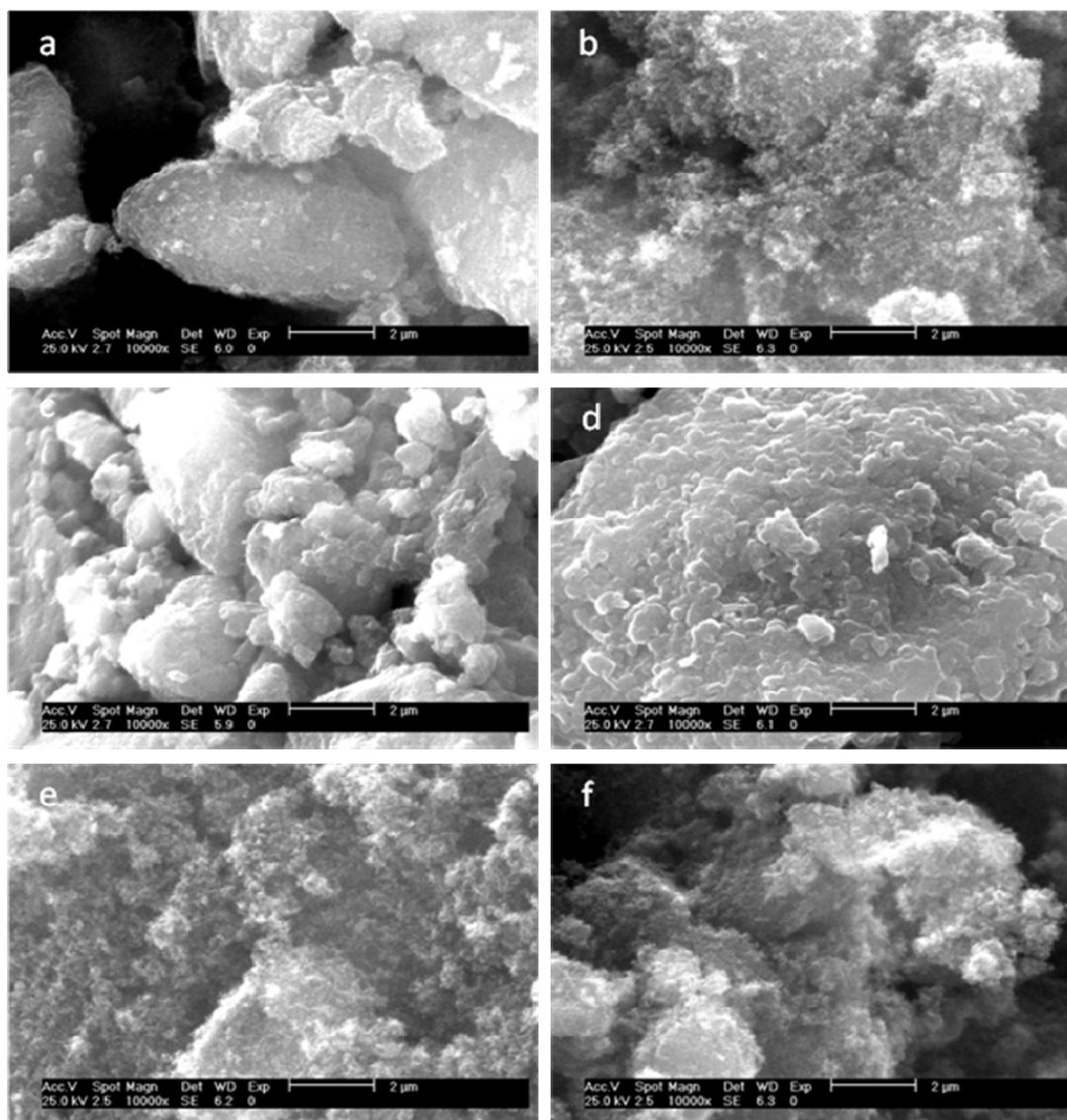


Figure 1. SEM images of a) Meso-C, b) Micro-CPANI, c) Meso-C/PANI1, d) Meso-C/PANI4, e) Micro-C/PANI1 and f) Micro-C/PANI4 composites.

2. EXPERIMENTAL

Two commercial activated carbons, a mesoporous-rich (Monarch 1400C) and a microporous-rich (BP2000), both obtained from Cabot, hereafter labeled as Meso-C and Micro-C were tested. Aniline monomer (Aldrich) was distilled prior to use and stored at 278K. Carbon/polyaniline composites were prepared by adsorption of aniline on the carbon surface followed by chemical polymerization. In a typical reaction, 2 g of carbon was added to 30 ml of an aqueous 1M HCl solution containing 0.5 g (5.37 mmol) of aniline. After stirring for 30 min, 30 ml of an aqueous 1 M HCl solution containing 1.227 g (5.37 mmol) of ammonium peroxodisulfate (Aldrich) was added dropwise at 273 K and stirring continued for 3 h. The resulting composites were filtered and washed with deionized water up to neutral pH, then dried at 313 K over P₂O₅ for 72h. The mass loading of PANI in the composite was evaluated by mi-

Table 1. Carbon/PANI composites composition

Sample	PANI Nominal content wt%	PANI Real content wt%
Meso-C/PANI1	20.0	18.6
Meso-C/PANI2	33.3	25.7
Meso-C/PANI3	50	39.0
Meso-C/PANI4	60	46.0
Micro-C/PANI1	20	16.1
Micro-C/PANI2	33.3	24.3
Micro-C/PANI3	50	35.1
Micro-C/PANI4	60	43.1

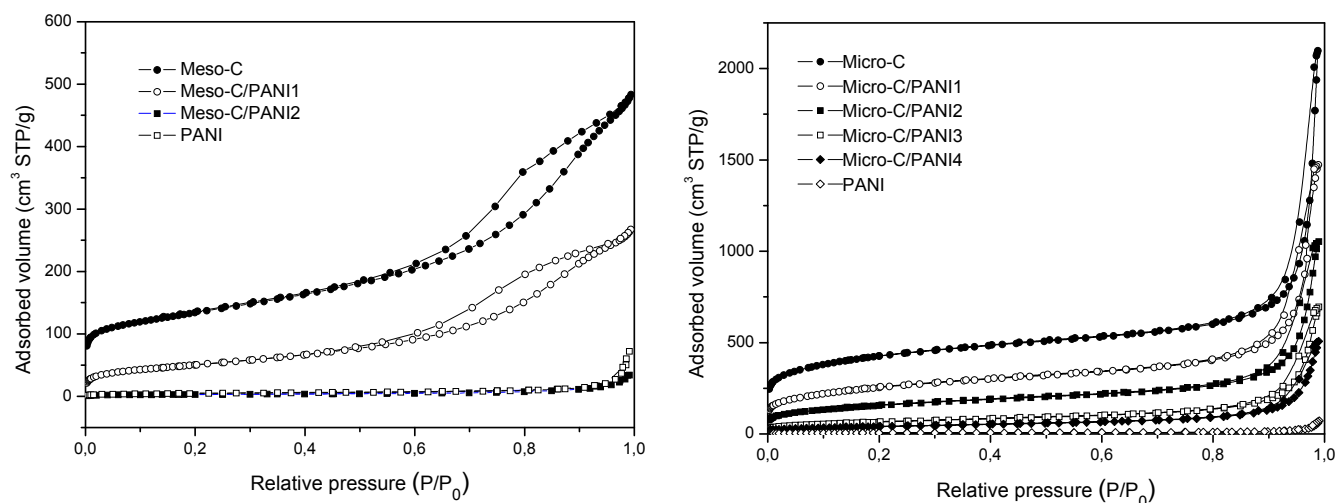


Figure 2. Nitrogen adsorption isotherms of Meso and Micro.C carbon/PANI composites.

croanalysis (LECO CHNS- 932).

The morphology of the carbon/PANI composites was characterized by scanning electron microscopy (Philips ESEM XL30) operating at 25 kV. Porosity of the composites was analyzed by N₂ adsorption at 77K (Micromeritics ASAP 2010). The apparent specific surface area was determined from the N₂-adsorption isotherm using the Brunauer-Emmett-Teller (BET) method [23]. The pore volume (V_{total}) was calculated by the single point method at $P/P_0 = 0.97$. The microporous surface area was obtained from the equation: $S_{mic} (m^2 \cdot g^{-1}) = 2000V_{N_2} (cm^3 g^{-1})/L_0 (nm)$, where L_0 represents the average micropore width [24]. Pore size distribution was calculated by means of the Kruk–Jaroniec–Sayari method [25] applied to the adsorption branch.

Supercapacitor electrodes were processed as cylindrical pellets (12 mm diameter, 0.5 mm height) by cold pressing a homogeneous mixture containing 70 wt% composite, 10 wt% Super P carbon and 20 wt% PVDF binder. Symmetrical supercapacitors were assem-

bled in Swagelok™-type cells, using a glassy microfiber paper (Whatman BS45) as separator and a 2M H₂SO₄ aqueous solution as electrolyte. Two stainless steel (A20 alloy) rods acted as current collectors. Room temperature cyclic voltammetry, constant current galvanostatic charge-discharge cycles and ac impedance were performed by using a Solartron 1480 potentiostat/galvanostat equipment, in the potential range 0-1V. Impedance measurements were performed in the frequency range of 500 kHz to 0.005 Hz.

3. RESULTS AND DISCUSSION

Table 1 shows composite composition obtained from microanalysis tests (N determination, average of three measurements). A small decrease on the PANI content in the composites regarding to the theoretical one was detected in all cases. SEM micrographs are shown in Figure 1. It can be seen that the both carbons exhibits a granular structure; after polymerization of PANI, the carbon/PANI materials show a much more smooth sur-

Table 2. Textural properties of carbon/PANI composites

Sample	$S_{BET} / m^2 g^{-1}$	$V_{total} / cm^3 g^{-1}$	$V_{mic} / cm^3 g^{-1}$	$V_{mes} / cm^3 g^{-1}$	$S_{mic} / m^2 g^{-1} (< 2 nm)$
Meso-C	471	0,75	0,18	0,57	254
Meso-C/PANI1	183	0,41	0,07	0,31	28,9
Meso-C/PANI2	20,2	0,08	0,01	0,01	1,77
Meso-C/PANI3	12,2	0,04	-	-	1,80
Meso-C/PANI4	4,7	0,02	-	-	1,04
Micro-C	1510	3,24	0,57	2,68	700
Micro-C/PANI1	930	2,28	0,32	1,96	320
Micro-C/PANI2	566	1,63	0,20	1,43	171
Micro-C/PANI3	237	1,08	0,08	0,99	47,3
Micro-C/PANI4	145	0,78	0,05	0,73	24,0
PANI	16,7	0,10	0,01	0,09	0,03

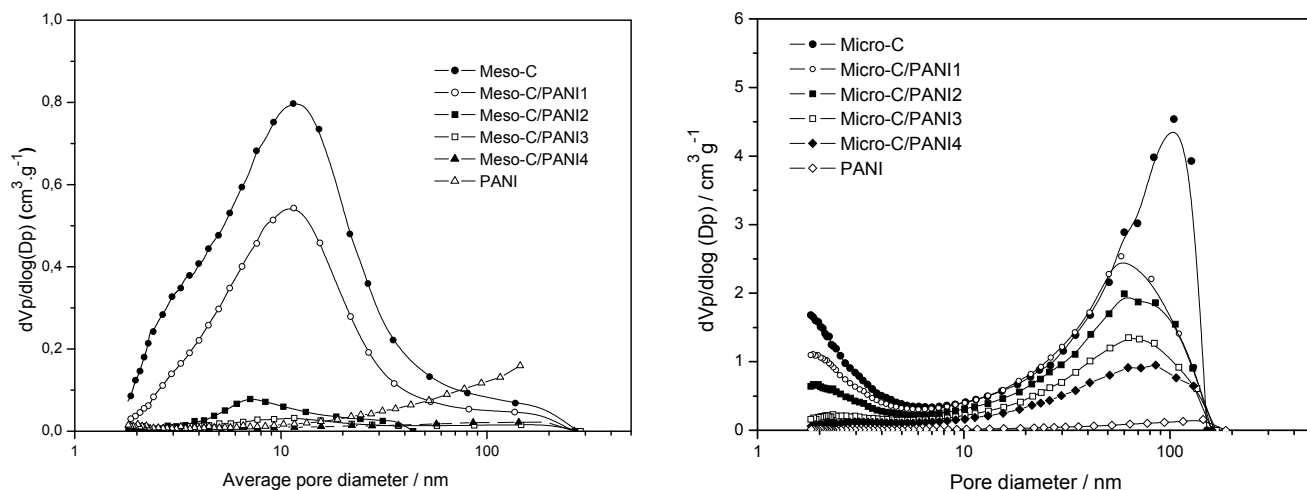


Figure 3. Pore-size distribution calculated for Meso and Micro-C carbon/PANI composites.

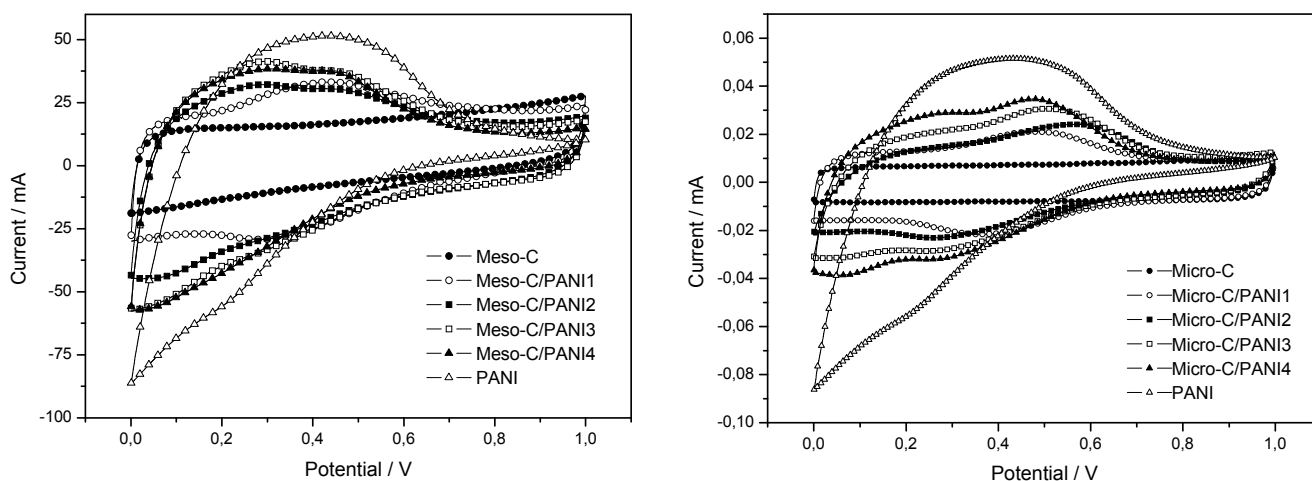


Figure 4. CV's of symmetric supercapacitors based on Meso and Micro-C/PANI composites measured at a scan rate of $10 \text{ mV}\cdot\text{s}^{-1}$. Potential window 0-1 V.

face, specially at high PANI loadings in the composite, due to the filling of the pores by the polymer. Figure 2 show the N_2 adsorption-desorption isotherms corresponding to carbons, polyaniline and the synthesized carbon/PANI composites. In terms of shape, the isotherm of both carbons can be classified as type IV according to the IUPAC, a hysteresis loop being observed on both isotherms in the range of ca. 0.6–1.0 P/P_0 for the Meso-C sample and 0.85–1.0 for the Micro-C carbon.

The textural characteristics of the samples calculated from nitrogen adsorption-desorption isotherms are listed in Table 2. Results indicate that the pore structure of the composites depends strongly on PANI concentration, the BET surface area decreasing from $471 \text{ m}^2\text{g}^{-1}$ calculated for the Meso-C to $4.7 \text{ m}^2\text{g}^{-1}$ for the composite with a 46 wt% PANI loading, due to the partial covering or filling of the pore structure of the carbon by the polymer. It is important to notice that the mesoporous structure of the carbon was maintained after PANI loading up to 20 wt%. The total pore volume also de-

creases when increasing PANI concentration, both mesopore and micropore structure being practically disappears for high PANI loadings. Similar effect was observed for Micro-C/PANI samples, but in this case the hysteresis, associated to the mesoporous pore structure was detected in all cases, independently of PANI concentration in the composite. Pore-size distribution of the samples, calculated by applying the Kruk-Jaroniec-Sayari branch of the isotherms, is shown in Figure 3. Meso-C carbon has a broad pore size distribution, with a maximum centered at 11.8 nm. Regarding the composites, the sample with the lower loading of PANI show a profile similar to that of the pristine carbon, with a maximum centered at 11.2 nm; increasing PANI loadings lead to a decrease on the pore size to 7.3 nm for the Meso-C/PANI2 sample, no pore being detected for higher PANI concentration. For Micro-C-based composites, the pore size distribution graph indicate the presence of macropores (pore diameter $>50 \text{ nm}$) in all samples, the pore volume again decreasing on increasing PANI concentration in

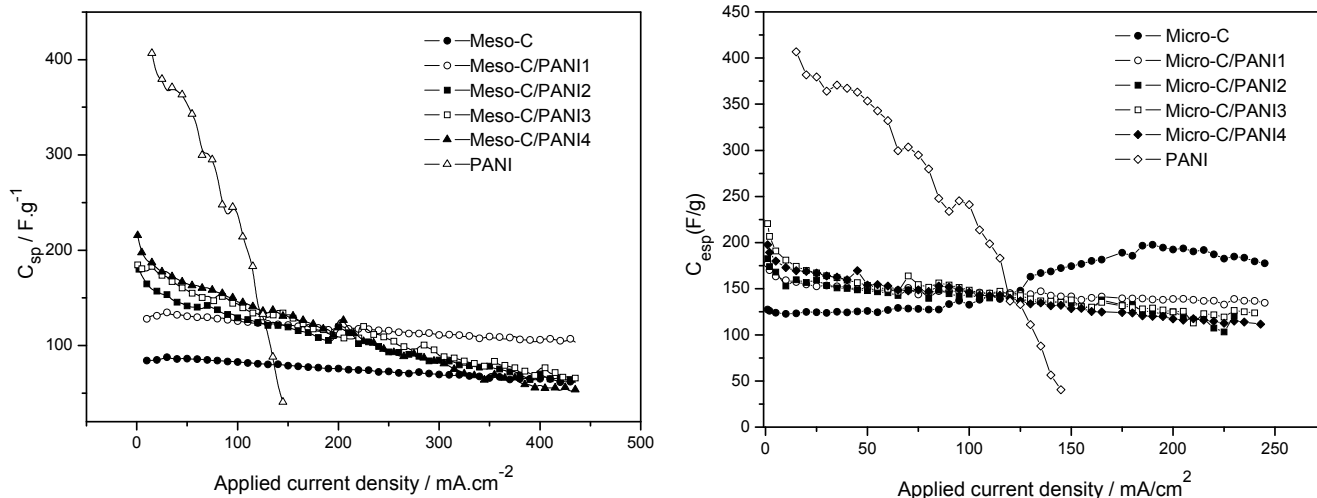


Figure 5. Discharge specific capacitance vs. applied current density of Meso C and Micro-C/PANI based symmetric supercapacitors. Potential window 0-1 V.

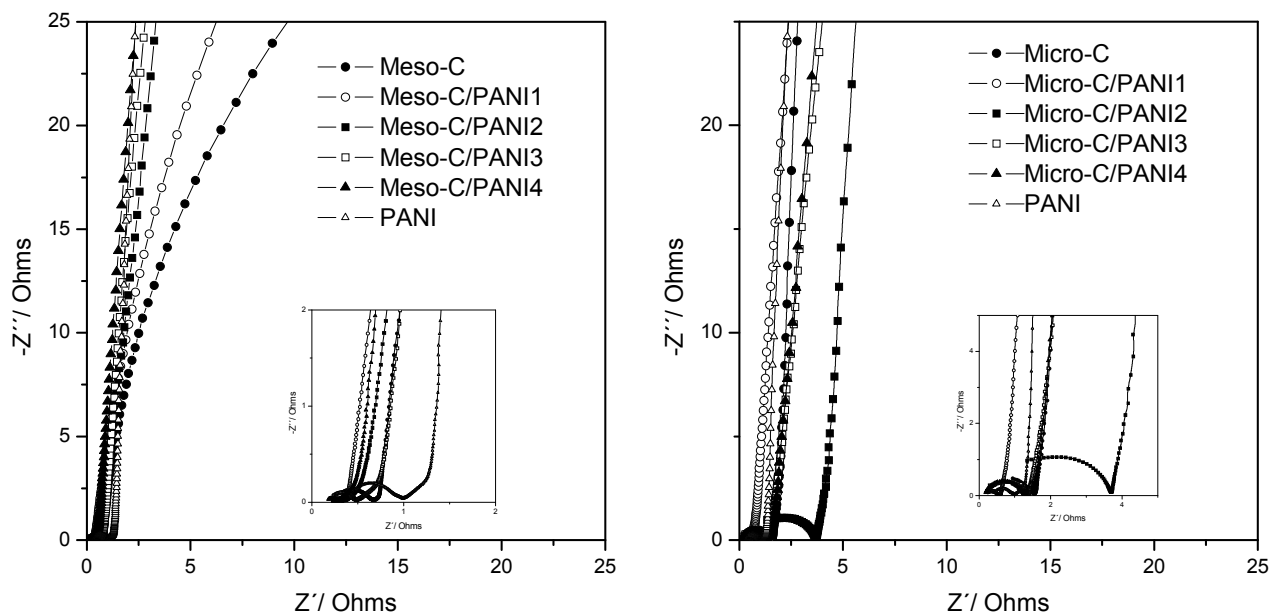


Figure 6. Nyquist plots for Meso and Micro.C carbon/PANI composite supercapacitors.

the composite.

Figure 4 shows the cyclic voltammograms of symmetric supercapacitors based on the Meso and Micro-C/PANI composites under study recorded at a scan rate of 10 mV.s⁻¹. Carbon-based devices cyclic voltammograms show the expected rectangular shape associated to an EDLC behavior, while deviations were detected for all composites, anodic and cathodic peaks being detected, associated to the redox transition of PANI between the semiconducting leucoemeraldine form to the conducting state (polaronic emeraldine form), and the emeraldine-pernigraniline transformation [26]. The current density increases gradually when increasing the scan rate, a positive shift of oxidation peaks and a negative shift of reduction

peaks being detected with the increase of the scan rate due to polarization.

Figure 5 show the variation of the specific capacitance, calculated from constant current galvanostatic charge/discharge test vs. the applied current density by using the expression:

$$C_{sp} = \frac{I\Delta t}{m\Delta V}$$

Where I is the discharge current (amperes), Δt is the discharge time (s), m is the mass of active material in the electrode (g) and ΔV is the potential range in the discharge process (V). The larger

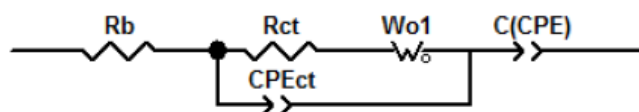


Figure 7. Equivalent circuit proposed to explain the behaviour of Meso and Micro-C carbon/PANI composite supercapacitors.

values of C_{sp} were obtained for the PANI-based device, but the value decrease sharply on increasing the applied current due to restrictions on the diffusion of the electrolyte anion, in this case SO_4^{2-} , (the doping agent). It is important to notice at this point that, while in EDLC supercapacitors the charge storage mechanism is restricted to the carbon surface, in redox devices is all the mass of the active material the responsible of the charge storage, and not only the surface, making diffusion of the ions of the electrolyte to inner of the material one of the limiting factors, especially when high current densities were applied. Meso-C/PANI composites show specific capacitance values that, at low applied current are higher than that of the pristine carbon, even part of the carbon pore structure was blocked by the polymer, but on increasing the applied current density the value of C_{sp} decreases, specially at high PANI loadings in the composite, again explained in terms of electrolyte ions diffusion restriction, that may even block the surface of the carbon to the electrolyte, making negligible the double layer contribution of the carbon surface to the overall charge storage process. This effect was observed in both Meso and Micro-C derived composites. For Meso-C composites, the best results were obtained for the electrode with the lower polyaniline loading (20 wt %), were the specific capacitance is 70% higher than that of the Meso-C carbon through all the range of applied current densities tested, while Micro-C electrodes. Looking at the results obtained can be postulated that for carbon/PANI composites, the best electrochemical properties, in terms of specific capacitance, will be obtained when using carbons with a mesoporous structure and low polyaniline loadings. The diffusion of the electrolyte ions, not only to the carbon surface, but also at the whole mass of the polymer is a key

factor in the charge storage process, especially for composites with high PANI loadings.

Figure 6 shows the room temperature complex-plane impedance plot of the symmetric supercapacitors based on the Meso and Micro-C/PANI composites under study. The inset in the figure shows the corresponding impedance behavior at high frequencies. The diagrams consist of a small semicircle at high frequencies, suggesting that the carbon particles are fully covered by the polymer, associated with the charge transfer resistance and capacity of the double layer, followed by a Warburg response at mid frequencies, and a vertical spike at low frequencies associated with the capacitive behavior of the electrode. The deviation of the vertical line observed for the Meso-C and Meso-C/PANI1 devices suggest that the charge storage process is diffusion-controlled, while surprisingly this effect was much lower for the Micro-C/PANI composites. The impedance plots may be represented by the equivalent circuit showed in Figure 7. Fitting of the experimental impedance data to the proposed equivalent circuit was made by using the ZView non-linear fitting software. The values of the circuit components are listed in Table 3. Bulk resistance (R_b) values, generally accepted as the summation of $R_{contact} + R_{electrolyte} + R_{bulk\ electrode} + R_{pore} + R_{separator}$, are low, ranging from 0.14 to 0.47 Ω , except for the Micro-C/PANI3 composite. The diameter of the semi-circle corresponds to the charge transfer resistance (R_{ct}). The larger value of R_{ct} detected for the Micro-C-based composites can be explained in terms of the blocking of the micropore structure, thus restricting the diffusion of the electrolyte to the carbon surface. The value of the equivalent series resistance (ESR), the result of $R_b + R_{ct}$, of Meso-C-based samples is lower than that of the Micro-C-based ones, and lower than the value corresponding to the pristine Meso-C carbon. If it was considered that the resistances of electrolyte, the separator, the pore structure and the contact resistances are identical in all the samples, this decrease can be explained in terms of the high electrical conductivity of the ES form of PANI in the composites. C_{dl} represents the double layer capacitance. The values of C_{dl} of all the samples are low, of the order of 10^{-4} to 10^{-3} Farads. The low frequency capacitance C represents not only pseudo-capacitance from PANI, which is attributed to the faradaic process of PANI redox transition, but the double layer capacitance from both PANI and the

Table 3. Parameters obtained from the non-linear fit of experimental impedance data to the proposed equivalent circuit

Sample	R_b / Ohms	R_{ct} / Ohms	C_{ct} / F	C / F
Meso-C	0.24	0.41	$3.30 \cdot 10^{-3}$	1.24
Meso-C/PANI1	0.23	0.08	$2.32 \cdot 10^{-3}$	1.23
Meso-C/PANI2	0.22	0.13	$2.89 \cdot 10^{-3}$	1.59
Meso-C/PANI3	0.20	0.26	$1.64 \cdot 10^{-4}$	2.03
Meso-C/PANI4	0.17	0.09	$1.29 \cdot 10^{-4}$	1.95
Micro-C	0.17	1.81	$3.52 \cdot 10^{-4}$	0.66
Micro-C/PANI1	0.16	0.37	$2.45 \cdot 10^{-4}$	1.09
Micro-C/PANI2	0.47	3.32	$4.29 \cdot 10^{-4}$	0.79
Micro-C/PANI3	1.14	1.20	$4.16 \cdot 10^{-4}$	0.94
Micro-C/PANI4	0.15	1.08	$1.99 \cdot 10^{-4}$	0.96
PANI	0.38	0.54	$1.98 \cdot 10^{-4}$	3.73

carbon. The value of the capacitance C of the Meso-C/PANI composites increase on increasing the PANI concentration, then decrease for the sample with the higher polymer concentration. For the Micro-C/PANI samples this relation is not so clear, the value of C calculated for the composites being in all cases higher than the one obtained for the unmodified carbon.

4. CONCLUSIONS

Meso and microporous carbon/polyaniline composites have been synthesized by the in-situ oxidative polymerization of aniline monomer on the surface of the carbon particles. Textural analysis indicate that composites porous structure depends strongly on the PANI content, S_{BET} and pore volume decreasing on increasing PANI concentration. Regarding supercapacitor performance, the best results, in terms of specific capacitance, were obtained for the Meso-C/PANI composite, the specific capacitance been 70% higher than that of the Meso-C carbon through all the range of applied current densities tested. The results obtained suggest that, for carbon/PANI composites, the best specific capacitance will be obtained when using carbons with a mesoporous structure and low polyaniline loadings. The diffusion of the electrolyte ions, not only to the carbon surface, but also at the whole mass of the polymer is a key factor in the charge storage process, especially for composites with high PANI loadings.

5. ACKNOWLEDGEMENTS

Financial support by the Spanish Ministry of Science and Innovation Project ENE2007-62791/ALT is gratefully acknowledged. M.A. Torre thanks for a contract associated with that project.

REFERENCES

- [1] A.F. Burke, T.C. Murphy, in "Proceedings of the Materials Research Society Symposium on Materials for Energy Storage and Conversion: Batteries, Capacitors and Fuel Cells", Eds. D.H. Goughly, B. Vyas, T. Takamura, J.R. Huff, Pittsburgh, USA, 1995.
- [2] S. Sarangapani, B.V. Tilak, C.P. Chen, J. Electrochem. Soc., 143, 3791 (1996).
- [3] C. Arbizzani, M. Mastragostino, B. Scosati in "Handbook of Organic Conductive Molecules and Polymers", vol. 4, Ed. H.S. Nalwa, Wiley, Chichester, UK, 1997.
- [4] B.E. Conway in "Electrochemical Supercapacitors", Kluwer Academic/Plenum, New York, USA, 1999.
- [5] K. Babel, K. Jurewicz, J. Phys. Chem. Solids, 65, 275 (2004).
- [6] A.B. Fuertes, G. Lota, T.A. Centeno, E. Frackowiak, Electrochim. Acta, 50, 2799 (2005).
- [7] J. Li, X.Y. Wang, Q.H. Huang, S. Gamboa, P.J. Sebastian, J. Power Sources, 158, 784 (2006).
- [8] E. Frackowiak, K. Jurewicz, S. Delpeux, F. Beguin, J. Power Sources, 97, 822 (2001).
- [9] H.H. Zhou, H. Chen, S.L. Luo, G.W. Lu, W.Z. Wei, Y.F. Kuang, J. Solid State Electrochem., 9, 574 (2005).
- [10] L.-Z. Fan, J. Maier, 1958, 937 (2006).
- [11] A. Laforgue, P. Simon, C. Sarrazin, J.-F. Fauvarque, J. Power Sources 80, 142 (1999).
- [12] J.H. Jang, A. Kato, K. Machida, K. Naoi, J. Electrochem. Soc., 153, A321 (2006).
- [13] Y.G. Wang, Y.Y. Xia, Electrochim. Acta, 51, 3223 (2006).
- [14] R.N. Reddy, R.G. Reddy, J. Power Sources, 124, 330 (2003).
- [15] J.H. Park, J.M. Ko, O.O. Park, D.W. Kim, J. Power Sources, 105, 20 (2002).
- [16] Q.F. Xiao, X. Zhou, Electrochim. Acta, 48, 575 (2003).
- [17] J. Jang, J. Bae, M. Choi, S.H. Yoon, Carbon, 43, 2730 (2005).
- [18] E. Frackowiak, V. Khomenko, K. Jurewicz, K. Lota, F. Beguin, J. Power Sources, 153, 413 (2006).
- [19] H.F. An, Y. Wang, X.Y. Wang, L.P. Zheng, X.Y. Wang, L.H. Yi, L. Bai, X.Y. Zhang, J. Power Sources, 195, 6994 (2010).
- [20] D. Bélanger, X. Ren, J. Davey, F. Uribe, S. Gottesfeld, J. Electrochem. Soc., 147, 2923 (2000).
- [21] K.S. Ryu, K.M. Kim, N.-G. Park, Y.J. Park, S.H. Chang, J. Power Sources, 103, 305 (2002).
- [22] H.H. Zhou, H. Chen, S.L. Luo, G.W. Lu, W.Z. Wei, Y.F. Kuang, J. Solid State Electrochem., 9, 574 (2005).
- [23] S. Brunauer, P. Emmet, E. Teller, J. Am. Chem. Soc., 60, 309 (1938).
- [24] H.F. Stoeckli in "Porosity in Carbons", Ed. J.W. Patrick, Edward Arnold, London, UK, 1995.
- [25] M. Jaroniec, A. Safari, Langmuir, 13, 6267 (1997).
- [26] C.C. Hu, J.Y. Lin, Electrochimica Acta, 47, 4055 (2002).